European Journal of Pharmaceutical Sciences 165 (2021) 105926

Contents lists available at ScienceDirect

European Journal of Pharmaceutical Sciences

journal homepage: www.elsevier.com/locate/ejps

Dosing-time dependent testicular toxicity of everolimus in mice

Narin Ozturk, PhD [a], Dilek Ozturk Civelek, PhD [b], Serap Sancar, PhD [c], Engin Kaptan, PhD [c], Zeliha Pala Kara, PhD [a], Alper Okyar, PhD [a,*]

[a] Department of Pharmacology, Faculty of Pharmacy, Istanbul University, Beyazit-Istanbul, Turkey
[b] Department of Pharmacology, Faculty of Pharmacy, Bezmialem Vakif University, Fatih-Istanbul, Turkey
[c] Department of Biology, Faculty of Science, Istanbul University, Vezneciler-Istanbul, Turkey

ARTICLE INFO

Keywords:
Everolimus
Testicular toxicity
Chronotoxicity
Biological rhythm
Circadian clock
Male mice

ABSTRACT

The circadian timing system controls many biological functions in mammals including drug metabolism and detoxification, cell cycle events, and thus may affect pharmacokinetics, target organ toxicity and efficacy of medicines. Selective mTOR (mammalian target of rapamycin) inhibitor everolimus is an immunosuppressant and anticancer drug that is effective against several cancers. The aim of this study was to investigate dosing-time dependent testicular toxicity of subacute everolimus administration in mice. C57BL/6 J male mice were synchronized with Light-Dark (12h:12 h) cycle, with Light-onset at Zeitgeber Time (ZT)-0. Everolimus (5 mg/kg/day) was administered orally to mice at $ZT1_{rest\text{-}span}$ or $ZT13_{activity\text{-}span}$ for 4 weeks. Body weight loss, clinical signs, changes in testicular weights, testis histology, spermatogenesis and proliferative activity of germinal epithelium of seminiferous tubules were examined. Steady-state everolimus concentrations in testes were determined with validated HPLC method. Everolimus toxicity was less severe following dosing at ZT13 compared to ZT1, as shown with least body weight loss ($p<0.001$), least reductions in testes weights ($p<0.001$) and least histopathological findings. Everolimus-induced histological changes on testes included vacuolisation and atrophy of germinal epithelium, and loss of germinal cell attachment. The severity of everolimus-induced histological toxicity on testes was significantly more evident in mice treated at ZT1 than ZT13 ($p<0.001$). Spermatogenic cell population significantly decreased when everolimus administered at ZT1 compared to ZT13 ($p<0.001$). Proliferative activity of germinal epithelium was significantly decreased due to treatment at ZT1 compared to ZT13 ($p<0.001$). Everolimus concentrations in testes indicated a pronounced circadian variation, which was greater in mice treated at ZT1 compared to ZT13 ($p<0.05$). Our study revealed dosing-time dependent testicular toxicity of everolimus in mice, which was greater in severity when everolimus administered at early rest-span (daytime-ZT1) than early activity-span (nighttime-ZT13). These findings support the concept of everolimus chronotherapy for minimizing reproductive toxicity and increasing the tolerability of everolimus, as a clinical advantage.

1. Introduction

The mammalian target of rapamycin (mTOR) inhibitors (i.e., sirolimus and everolimus) are the cornerstones of most immunosuppressive protocols used in kidney, heart and liver transplant recipients to prevent organ rejection (Klawitter et al., 2015; Manito et al., 2010). In addition to its immunosuppressant effects and ability to prolong graft survival in patients, everolimus (RAD001) is also used as an antitumor agent in cancer treatment with its proliferation signal inhibitory effects (Booth et al., 2010; Lebwohl et al., 2013). It is approved for various conditions including advanced renal cell carcinoma, progressive pancreatic neuroendocrine tumors, advanced hormone-receptor positive, HER2-negative breast cancer in post-menopausal women in combination with exemestane (Booth et al., 2010; Lebwohl et al., 2013).

Everolimus which is the 40-O-(2-hydroxyethyl) derivative of sirolimus is an orally administered, selective mTOR inhibitor (Booth et al., 2010; Klawitter et al., 2015). mTOR is a key serine-threonine kinase in the phosphoinositide 3-kinase (PI3K)-AKT-mammalian target of rapamycin (PI3K/AKT/mTOR) signaling pathway which plays a pivotal role in the regulation of protein synthesis associated with cell growth and proliferation, angiogenesis, cellular metabolism and autophagy as well as the regulation of the immune response. mTOR signaling pathway is known to be dysregulated in the majority of human cancers. Therefore mTOR inhibition is an important antitumor target (Booth et al., 2010;

* Corresponding author at: Department of Pharmacology, Faculty of Pharmacy, Istanbul University, 34116 Beyazit-Istanbul, Turkey.
E-mail address: aokyar@istanbul.edu.tr (A. Okyar).

https://doi.org/10.1016/j.ejps.2021.105926
Received 4 March 2021; Received in revised form 13 June 2021; Accepted 4 July 2021
Available online 7 July 2021

Fasolo and Sessa, 2008; Lebwohl et al., 2013; Leighton et al., 2009).

Everolimus treatment is associated with numerous side effects. It has been reported that patients treated with everolimus mostly suffered from fatigue, stomatitis, body weight loss, proteinuria, peripheral edema, pneumonitis, decreased hematology parameters, metabolic abnormalities such as hypercholesterolemia, hyperglycemia and increased liver enzymes (Booth et al., 2010; Lebwohl et al., 2013; Leighton et al., 2009). General toxicology studies have revealed that everolimus associated toxicities were commonly observed in the male reproductive system, lymphoid tissues, lungs, gastrointestinal tract, coagulation pathways, metabolism and endocrine system (Booth et al., 2010; Leighton et al., 2009). Studies have shown a potential negative impact of mTOR inhibitors on male reproductive system (Boobes et al., 2010; Chen et al., 2013; Deutsch et al., 2007; Huyghe et al., 2007; Rovira et al., 2012). In a recent study, it has been demonstrated that long-term oral treatment of mTOR inhibitor sirolimus at the dose equivalent to the therapeutic levels used for post-renal transplant patients has considerably affected testicular development and gonadal function accompanied by significant histological changes of testicular structures in rats (Chen et al., 2013). Reproductive toxicology studies indicate that treatment of everolimus has detrimental effects on the testis and impairs gonadal functions (Booth et al., 2010; Huyghe et al., 2007; Leighton et al., 2009). In a preclinical study, everolimus caused infertility in male rats, with only partial recovery after 10–13 weeks of treatment-free period, and adverse effects on male reproductive organs were not completely recovered (Leighton et al., 2009).

In mammals, many biological functions involved in organism physiology, biochemistry and behavior are governed by the Circadian Timing System (CTS) over a 24-h period. The CTS is composed of molecular clocks located in each nucleated cells which drive 24-h (circadian) changes in xenobiotic metabolism and detoxification, hormone secretion, body temperature, blood pressure, immune system activity, cell proliferation and apoptosis as well as many other physiological processes (Lévi et al., 2010; Mohawk et al., 2012; Ohdo et al., 2019). Almost half of the protein-coding genes in mammals display circadian dependent transcription (Lévi et al., 2010; Ohdo et al., 2019). Circadian rhythms of biological functions in the organism may affect the pharmacokinetic and pharmacodynamic processes of many drugs. Thus, drugs may vary in efficacy and/or target organ toxicity related with the rhythmicity of biochemical, physiological and behavioral processes under the control of the circadian clock (Dallmann et al., 2016; Filipski et al., 2014; Lévi et al., 2010; Ohdo et al., 2019; Ozturk et al., 2017). Preclinical and clinical studies carried out so far have shown that the efficacy, tolerability and extent of toxicity of many drugs, especially used in cancer treatments, may be profoundly modified by changing the timing of administration along the 24-h time scale (i.e. circadian timing) in both experimental models and in patients. Li et al. showed that both tolerability and efficacy of gemcitabine were better when administered during the early active phase as compared to the late active phase (Li et al., 2005). In a clinical study, it was demonstrated that treatment with gemcitabine at 9:00 AM (early active phase of human) decreased the toxicity on white blood cells (WBC) and platelets by nearly 10% as compared to treatment at 15:00 (Iwata et al., 2011). Irinotecan chronotoxicity was also shown to be correlated in experimental animals and cancer patients. Okyar et al. indicated that best tolerability time of irinotecan ileum toxicity in mice was at ZT11–15 (active phase of mice) (Okyar et al., 2011). Similar to animal studies, clinical study results support irinotecan administration in the morning for males and in the afternoon for females, in order to minimize adverse effects without impairing efficacy (Innominato et al., 2020). The myelotoxic effects of oxaliplatin (L-OHP) were attenuated when mice were injected with this drug during the dark phase (Kato et al., 2020). In a clinical study, a lower incidence of severe diarrhea and neutropenia with chrono-modulated IFLO5 (5-fluorouracil-leucovorin, peaking at 04:00 AM at night, and oxaliplatin, peaking at 4:00 PM) chemotherapy in comparison with conventional administration (Innominato et al., 2020). Increased efficacy has seen when drugs are given near their times of best tolerability (Bicker et al., 2020; Binkhorst et al., 2015; Lévi et al., 2010; Ohdo et al., 2019; Ozturk et al., 2018; Sancar and Van Gelder, 2021). Hence, chronopharmacological studies have been of importance in determining the most appropriate drug administration time of the day to optimize drug therapy.

Since adverse effects related to long-term everolimus exposure are deleterious to the patient quality of life and compliance, circadian timing of this drug could improve tolerability and decrease the target organ toxicity in patients. As yet, we lack information for circadian time-dependent effects of everolimus on the male reproductive system. The present study was designed to investigate the dosing-time dependent testicular toxicity of subacute everolimus administration in mice.

2. Materials and methods

2.1. Animals and their synchronization

8–10 weeks old, male C57BL/6 J mice (20–25 g body weight) were purchased from Istanbul University Aziz Sancar Institute of Experimental Medicine. Mice were housed in cages up to five animals in the room equipped with temperature control (22±2 °C) and humidity (55±5%). Water and food were provided ad libitum throughout the experiments. Mice were synchronized for 4 weeks with 12 h of light (L) in alternation with 12 h of darkness (D) (LD 12:12 h Light/Dark cycles) prior to any intervention and the same lighting regimen continued to the end of the experiment. All the manipulations during dark span were performed under dim red light (7×10^{4} erg/cm^2). Experiments were conducted in accordance with the guidelines approved for animal experimental procedures by the Istanbul University Local Ethics Committee of Animal Experiments (IUHADYEK, Approval No: 2014/12; BVU-HADYEK, Approval No: 2015/125).

2.2. Drugs and reagents

Everolimus (RAD001) was purchased from ApexBio Technology (Houston, Texas, USA). Drug was dissolved in propylene glycol:water (50:50, v/v) on each study day to prepare freshly, prior to oral gavage. The drug was orally administered to the mice in a fixed fluid volume (10 mL/kg body weight). Solvents were reagent grade and all other commercially available reagents were used as received unless otherwise stated.

2.3. Experimental study design

Everolimus was administered to synchronized male mice (5 mg/kg/day, $n = 8$/ZT) orally at ZT1 and ZT13 for 4 weeks. Control mice ($n = 5$/ZT) were only treated with vehicle (propylene glycol:water; 50:50, v/v) orally. Male mice were divided into 4 groups: ZT1C (vehicle treatment to mice at ZT1, control group, $n = 5$), ZT1E (everolimus treatment to mice at ZT1, $n = 8$), ZT13C (vehicle treatment to mice at ZT13, control group, $n = 5$), ZT13E (everolimus treatment to mice at ZT13, $n = 8$). ZT0 (Zeitgeber Time 0) means light onset, which corresponds to the beginning of the rest phase of the mice. ZT12 is time of lights off which corresponds to the beginning of the active phase. Everolimus administration times ZT1 and ZT13 were selected according to our findings of previous experiments (Ozturk et al., 2014). Everolimus dose was determined according to the previous studies on the literature and based on our findings of preliminary experiments in mice (Fasolo and Sessa, 2008; Huynh et al., 2009; Ozturk et al., 2014). Everolimus was preferred to given for 28 days (subacute) to see the dosing-time dependent toxic effects of repeated-dose administration.

Body weight was measured every day as an index of general toxicity. Drug induced body weight change was expressed relative to body weight on the initial treatment day. Throughout the study, animals were monitored for mortality, clinical symptoms, food and water

consumption, and behavioral signs. One day after the last dose, mice were sacrificed by cervical dislocation. Testes and other major organs (liver, kidneys, lungs) were removed and weighed. Testis tissues were processed for histological, immunohistochemical and HPLC analyses.

2.4. Histological evaluation

Testis tissues were weighed and the organ/body weight indexes were calculated using the following formula: Organ/Body Weight Index= (Organ Weight / Body Weight) x 100. Then, tissues were fixed in Bouin's solution, washed with 70% ethanol to remove picric acid, dehydrated in a series of graded ethanol and embedded in paraffin. Sections of 5 μm thickness were taken serially and stained with Hematoxylin-Eosin (H&E) and Masson's triple stain. Sections were evaluated histologically using light microscope (Olympus, Cx23, Tokyo, Japan) and photomicrographs were taken using a photomicroscope (Olympus, Bx53, Tokyo, Japan) at a magnification of x200. Histological damage score was determined for testis tissues using the criteria such as vacuolisation of germinal epithelium, loss of germinal cell attachment, and atrophy of germinal epithelium. The histological damage was scored on testis tissues and graded as follows: 0-absence, 1-very rare, 2-weak, 3-moderate and 4-severe. Scoring of each tissue sample represent the mean score of ten different sections.

2.5. Evaluation of spermatogenesis

Spermatogenesis was evaluated by counting the cells constituent seminiferous tubule (ST) wall. Among these cells, Sertoli cells (SC) are somatic cells which play an important role in the regulation of spermatogenesis. The others are germ cells at various stages of differentiation and consist of spermatogonia (SPG), spermatocytes (SPC) and spermatids (SPT). Five randomly selected STs were considered in order to count the cells in a hematoxylin-stained testis section. Mouse ST cells were identified according to the publication by Meistrich & Hess (2013). Briefly, SC located in the seminiferous epithelium and attached to the tubular basal lamina were identified as a pear-shaped nucleus. Spermatogonia were located in the basement membrane of the ST and identified as larger and almost round shape nuclei. Spermatocytes were detected by their larger size and deeply stained nuclei. Spermatids were apparent by different size and shape. They were counted considering their two different morphology, round (rSPT) and elongated spermatids (eSPT).

2.6. Proliferating cell nuclear antigen (PCNA) immunohistochemistry

The paraffin sections were deparaffinised in xylene, rehydrated in a decreasing ethanol series and rinsed in distilled water. After antigen retrieval using 10 mM citrate buffer (pH 6.0), the endogenous peroxidase activity was blocked with 3% (v/v) H_2O_2 for 15 min in the sections. Subsequently, sections were incubated with blocking serum for 15 min at room temperature in order to prevent nonspecific antibody binding. Afterwards, the sections were incubated with mouse monoclonal anti-PCNA antibody (1:50, Santa Cruz, TX, USA) for 30 min at room temperature. Streptavidin-biotin system (Thermo Fisher Scientific, MA, USA) was used to detect antibody binding. According to instruction of the manufacturer, sections were incubated with biotinylated secondary antibody for 30 min, rinsed in phosphate buffered saline (PBS) and incubated with horseradish peroxidase conjugated streptavidin for 30 min at room temperature. The peroxidase activity was visualized with 3-amino-9-ethylcarbazole (AEC). The sections were counterstained with Mayer's hematoxylin, mounted in Glycerol Vinyl Alcohol (GVA) and observed using an Olympus BX53 microscope (Tokyo, Japan). The proliferative index were calculated using the ratio between stained cell number and total cell number (Stained Cell Number / Total Cell Number x 100).

2.7. Analysis of steady-state everolimus concentrations in testis tissues by HPLC/UV

Everolimus (5 mg/kg/day) was perorally administered to male mice for 14 days to reach the steady-state concentration in testis tissue according to elimination half-life of everolimus. 24 h after the last dose, mice were sacrificed and testis tissues were isolated. 200 μl of 0.25 M zinc sulfate (1:9 water:methanol: v/v) solution containing repaglinide (10 μg/mL) as internal standard was added to the test tubes containing the testis samples and vortexed for 1 min. Then, the tissues were lysed with an ultrasonic homogenizer (Sonopuls, Germany) and centrifuged at 4000 rpm for 10 min. The supernatant was filtered through 0.45 μm nylon filters, taken into vials containing microinsert and injected into the column as 40 μl. Shimadzu HPLC system (Kyoto, Japan) with LC-30AD pump and SPD-20A UV/VIS detector was used for the bioanalytical determination of everolimus from the testis tissues. Chromatographic seperation was carried out on C8 column (100 × 4.6 mm, 5 μm, Phenomenex, USA) using acetonitrile:ammonium acetate buffer (60:40, v/v, pH 4.0) isocratically at a flow rate of 1 ml/min. The chromatographic peak were detected via UV dedector at 278 nm. Steady-state everolimus concentrations in testis tissues were calculated from the standard curve and given as μg/g.

2.8. Statistical analysis

Data were expressed as mean ± standard error of the means (SEM) for each studied variable. Statistical analyses were performed using GraphPad Prism 8.00 for Windows (GraphPad Software, CA, USA). Statistical significance between the means of different groups was validated with Student *t*-test or two-way analysis of variance (ANOVA) followed by Tukey's multiple comparison. A p value less than 0.05 was used to determine the level of statistical significance.

3. Results

3.1. General toxicity

General toxicity of everolimus was assessed on the basis of mortality, general behavior, clinical signs, and changes in body and organ weights in mice. Everolimus treatment resulted in dosing time-dependent body weight loss (15.0% decrease in mean body weight compared to the initial treatment day) in ZT1E group ($p<0.01$), while only a decrease in body weight gains were observed in ZT13E. Mean body weights of mice measured before the treatment with vehicle or everolimus (on day 0) and after 28-day treatment (on day 29, the day after the last dose) were given in Table 1, as shown in our previous study (Ozturk et al., 2018). Changes in organ weights due to everolimus administration at ZT1 and ZT13 were examined as an index of overall toxicity, and significant differences in relative organ weights between groups were found as a function of dosing-time. Liver, kidney and lung weights were increased upon everolimus treatment, whereas a decrease was observed in testes weights, and all the changes were more evident in mice treated with everolimus at ZT1 compared to ZT13. Table 1 summarizes the changes in body weights and relative organ weights after 4-week everolimus exposure. When general well-being of the mice were observed by clinical signs and behavioral assessment, apparent differences were found between ZT1E and ZT13E. Slight dyspnea, slight to moderate ruffled fur and decreased activity were observed in ZT1E group, whereas no clinical signs were observed in ZT13E.

3.2. Histological toxicity

Subacute everolimus treatment resulted in significant reductions in the testes weights of mice at both ZT1E and ZT13E groups as compared to their controls. Everolimus treatment decreased the testis weight by about 58.6% ($p<0.001$) in ZT1E group as compared to ZT1C, and the

Table 1
Changes in body weights and relative organ weights after 4-week exposure to everolimus as an index of overall toxicity in mice.

Groups	ZT1C $n = 5$	ZT1E $n = 8$	ZT13C $n = 5$	ZT13E $n = 8$
Body Weight (g) (Before)	21.8 ± 1.15	22.2 ± 0.96	21.1 ± 0.72	22.6 ± 0.77
Body Weight (g) (After)	24.05±0.95	18.86±1.03$^{**, \#}$	23.20±1.02	22.81±0.90
Right Testes (mg/g)	3.94±0.26	1.64±0.07$^{****, \#\#}$	4.08±0.26	2.34±0.07****
Left Testes (mg/g)	3.88±0.12	1.58±0.03$^{****, \#\#\#\#}$	4.05±0.16	2.39±0.05****
Liver (mg/g)	53.43±1.79	57.48±1.93$^{\#\#\#\#}$	47.43±0.80	46.36±1.18
Kidneys (mg/g)	10.66±0.24	11.64±0.24	11.00±0.30	11.38±0.21
Lungs (mg/g)	6.18±0.55	7.52±0.20$^{*, \#\#\#}$	5.57±0.16	5.73±0.15

Data are presented as mean±SEM. Body weights of mice are given as measurement of before treatment (with vehicle or everolimus), i.e. on day 0, and after treatment on day 29, the day after the last dose. Organ weights are presented as organ-to-body weight ratios (mg/g). The weights of kidneys and lungs are expressed as the sum of the right and left organs. ZT1C: Vehicle-treated mice at ZT1; ZT1E: Everolimus-treated mice at ZT1; ZT13C: Vehicle-treated mice at ZT13; ZT13E: Everolimus-treated mice at ZT13. *, significantly different from its control #, significant difference between ZT1E and ZT13E. Two-way ANOVA with Tukey post hoc test (*. $^{\#}$ $p<0.05$, $^{**\#\#}$ $p<0.01$, $^{***\#\#\#}$ $p<0.001$ and $^{****\#\#\#\#}$ $p<0.0001$).

decrease was 41.8% ($p<0.001$) in ZT13E. The reduction was more evident in mice received everolimus at ZT1 than the ones at ZT13, with statistically significant difference (31.6%, $p<0.001$) (Fig. 1A).

Control tissue sections of testes exhibited well-organized histoarchitecture when compared to everolimus-treated groups. Drug-induced histological changes on testes included vacuolisation of germinal epithelium, loss of germinal cell attachment and atrophy of germinal epithelium (Fig. 1B). When we compared everolimus-treated experimental groups (ZT1E and ZT13E) to those of their controls, the histological changes that we detected by considering the evaluation score of testes were apparently observed both in ZT1 ($p<0.001$) and ZT13 ($p<0.001$), as shown in Fig. 1C. There were dramatic differences between ZT1E and ZT13E groups in the pathological morphology of testis which was more evident when everolimus administered to mice at ZT1 than ZT13 ($p<0.001$).

3.3. Spermatogenesis

Total cell number of ST wall decreased significantly in both ZT1E and ZT13E groups when compared to their controls. However, the decrement in the cell number was more evident in ZT1E group than ZT13E (87.40±15.26 vs 204.93±20.51 respectively, $p \leq 0.001$) (Fig. 2A). Decrease in spermatogenic cells such as SPC and SPTs in ZT1E and ZT13E groups likely contributed to total cell decrease in ST (Fig. 2B-2C). While number of SC and SPG did not change significantly, SPC, rSPT and eSPT, were markedly decreased in ZT1E and ZT13E groups as compared to their control groups (ZT1C vs. ZT1E, SPC: 55.60±11.13 vs. 23.66±8.28 $p<0.01$, rSPT: 82.35±11.95 vs. 38.71±14.18 $p<0.01$, eSPT: 112.05±15.97 vs. 1.66±3.03 $p<0.01$; ZT13C vs. ZT13E, SPC: 60.15±7.98 vs. 39.33±8.27 $p<0.01$, rSPT: 89.50±11.49 vs. 61.57±7.94 $p<0.01$, eSPT: 110.25±9.73 vs. 79.97±14.15 $p<0.01$, respectively). In addition, the number of SPC and SPTs in ZT1E group were lower than ZT13E. Especially, the number of eSPT were dramatically decreased in ZT1E compared to ZT13E and control groups (ZT13E vs. ZT1E, SPC: 39.33±8.27 vs. 23.66±8.28 $p<0.01$; rSPT: 61.57±7.94 vs. 38.71±14.18 $p<0.01$; eSPT: 79.97±14.15 vs. 1.66±3.03 $p<0.01$, respectively).

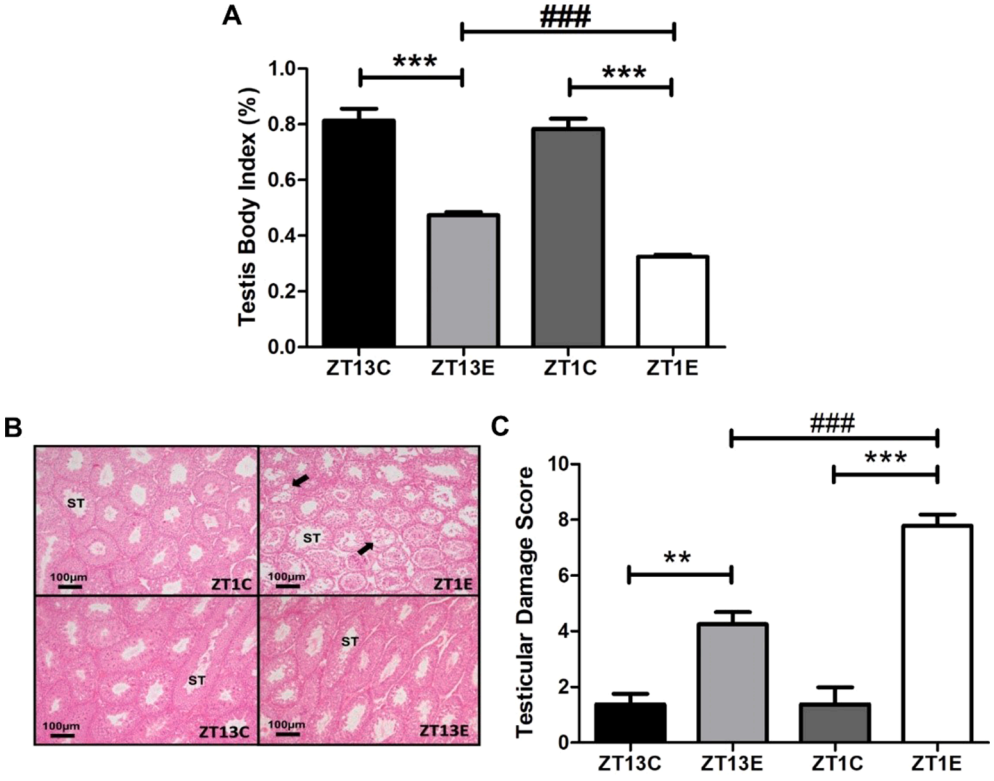

Fig. 1. Histological evaluation of dosing-time dependent testicular toxicity of everolimus and distribution in testis tissue. Data are mean±SEM. ZT1C: Vehicle-treated mice at ZT1; ZT1E: Everolimus-treated mice at ZT1; ZT13C: Vehicle-treated mice at ZT13; ZT13E: Everolimus-treated mice at ZT13, n = 5–8 for each group. **(A) Testis Body Index (%).** ZT13C: 0.81±0.04, ZT13E: 0.47±0.01, ZT1C: 0.78 ± 0.04, ZT1E: 0.32±0.01. The weights of testes are expressed as the sum of the right and left organs **(B) Everolimus-induced histological changes in testis tissue as a function of dosing-time.** Everolimus-induced histological changes on testes which was more evident in 1ME than 13 ME included vacuolisation of germinal epithelium, loss of germinal cell attachment and atrophy of germinal epithelium. Arrows indicates atrophy of germinal epithelium. **(C) Testicular Damage Score.** ZT13C: 1.38±0.75, ZT13E: 4.26 ± 1.14, ZT1C: 1.38±1.21, ZT1E: 7.79±1.07. *, significantly different from its control; $^{\#}$, significant difference between ZT1E and ZT13E. Two-way ANOVA with Tukey post hoc test (** $p<0.01$ ve $^{***, \#\#\#}$ $p<0.001$).

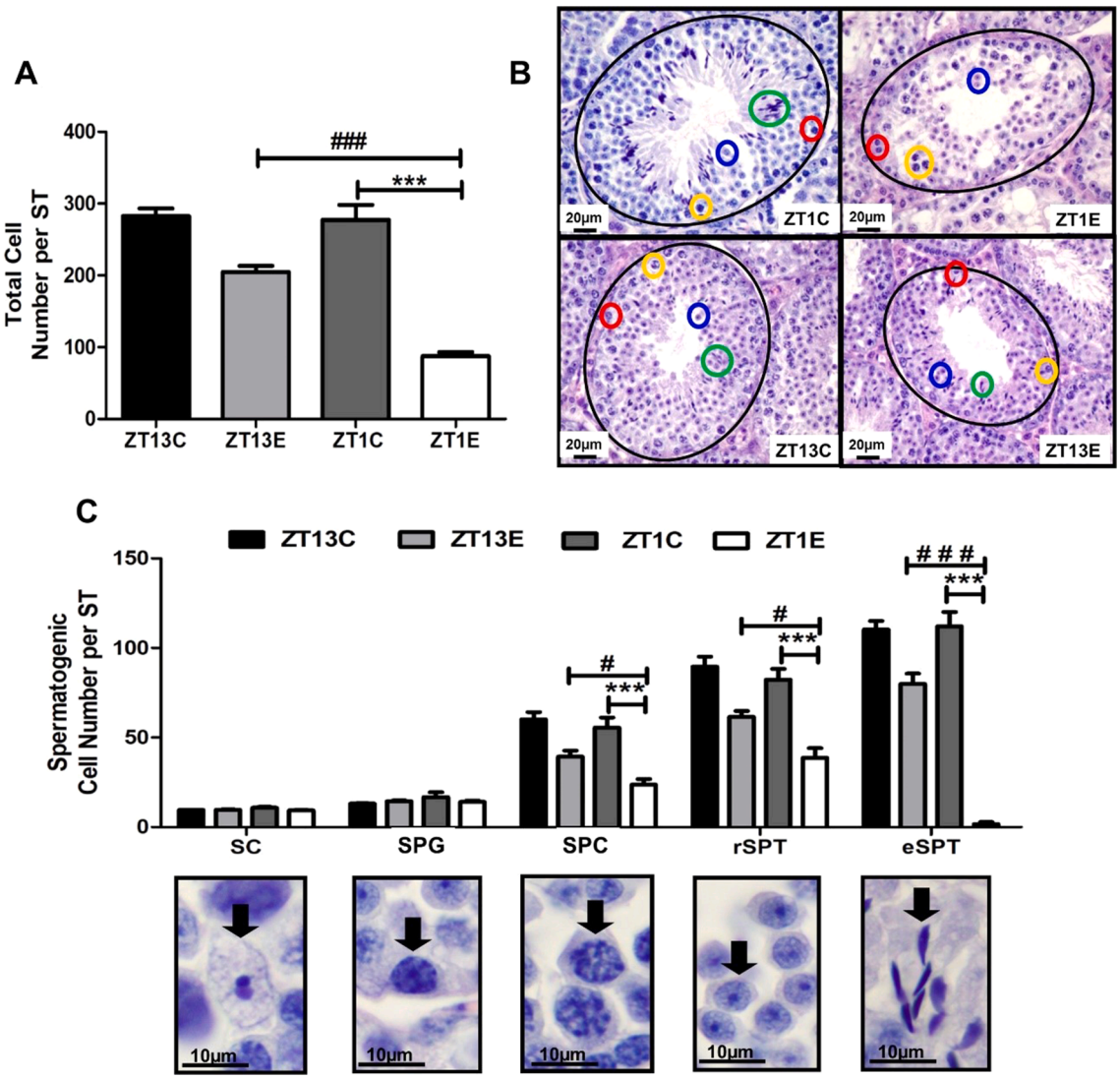

Fig. 2. Dosing-time dependent effect of everolimus on spermatogenesis in mice. ZT1C: Vehicle-treated mice at ZT1; ZT1E: Everolimus-treated mice at ZT1; ZT13C: Vehicle-treated mice at ZT13; ZT13E: Everolimus-treated mice at ZT13. **(A) Total number of the tubular epithelial cells per seminiferous tubules (ST). (B) Histological sections of ST in different experimental groups.** Red circle: SPG, yellow circle: SPC, blue circle: rSPT, green circle: eSPT. **(C) The number of various cell types in the germinal epithelium of ST**. The number of Sertoli cells (SC), spermatogonia (SPG), spermatocytes (SPC), and round (rSPT) and elongated spermatids (eSPT) in the germinal epithelium of different experimental groups. The cell numbers represent cell number per seminiferous tubules and five seminiferous tubule sections per animal in each group were randomly selected and analyzed. Two-way ANOVA with Tukey post hoc test (*** $p<0.001$ ZT1C vs. ZT1E, $^{\#}$ $p<0.05$, $^{\#\#\#}$ $p<0.001$ ZT13E vs. ZT1E).

3.4. Proliferation index in seminiferous tubules

Proliferative activity of germinal epithelium of seminiferous tubules during different circadian times was shown by using PCNA antibody indicating the S phase of the cell cycle. PCNA is a functional and structural player in DNA replication forks. The proliferation index is presented in Fig. 3A for the different circadian times. Generally, we detected proliferating cells with red nuclei in basal layer of the germinal epithelium (Fig. 3B). The index was the lowest in ZT1E group ($p<0.01$). The distribution of proliferative cells in the germinal epithelium did not evidently change among the other groups ZT1C, ZT13C and ZT13E. However, proliferative activity in ZT1E and ZT13E was significantly different between each other ($p<0.001$).

3.5. Effects of dosing-time on the distribution of everolimus in the testis

Everolimus showed dosing time-dependent distribution profile in testis tissue. Steady-state everolimus concentration in testis tissue was determined as 5.91±0.49 µg/g when mice treated at ZT1, while it was 4.09±0.66 µg/g at ZT13. Testis concentration of everolimus was 44.5% higher at ZT1-treated grup than ZT13 ($p<0.05$). Dosing-time dependent steady state concentrations of everolimus were given in Fig. 4.

4. Discussion

There has been a growing concern that mTOR inhibitors may increase the risk of infertility (Boobes et al., 2010; Deutsch et al., 2007; Huyghe et al., 2007). Knowledge of short- and long-term benefits and side/toxic effects of everolimus in its various uses as immunosuppressant and anti-tumor agent, and its clinical impact on reproductive system still remain unclear. The present study is the first to report the dosing time-dependent testicular toxicity of everolimus in mice. We observed a prominent administration time-dependent toxicity findings as assessed with the changes in organ / body weights, clinical signs spermatogenesis and histopathology. Our findings indicated that general toxicity for everolimus was least following dosing at ZT13.

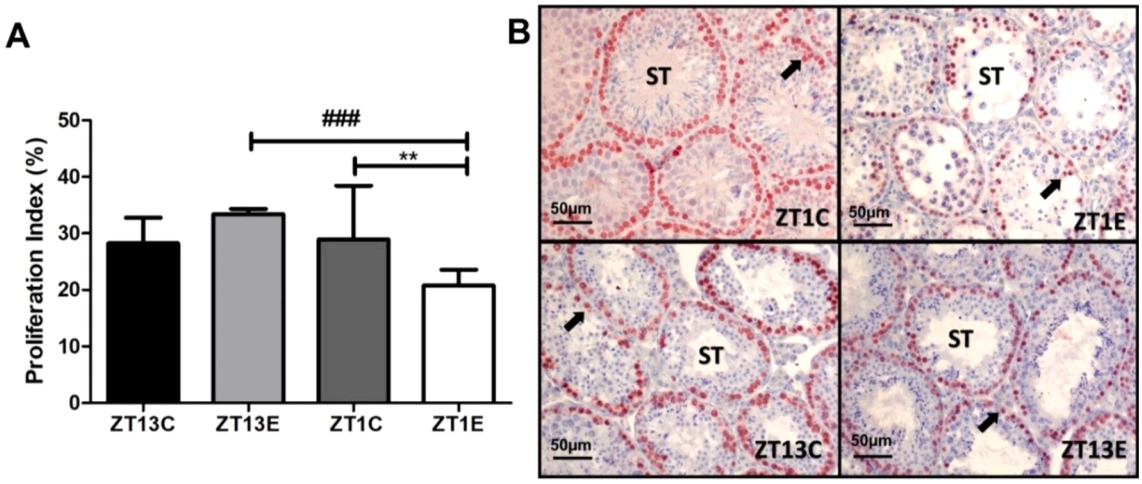

Fig. 3. Proliferative activity of testis due to dosing-time of everolimus at the different circadian times. ZT1C: Vehicle-treated mice at ZT1; ZT1E: Everolimus-treated mice at ZT1; ZT13C: Vehicle-treated mice at ZT13; ZT13E: Everolimus-treated mice at ZT13, $n = 5–8$ for each group. **(A) Proliferation Index (%).** Data are expressed as mean±SEM. ZT13C: 33.61±4.5; ZT13E: 32.66±0.9; ZT1C: 35.53±9.5; 1ME: 20.32±2.7; *, significantly different from its control; $^{\#}$, significant difference between ZT1E and ZT13E. Two-way ANOVA with Tukey post hoc test (** $p<0.01$ and$^{\#\#\#}$ $p<0.001$). **(B) Histological sections of the testis immunestained with PCNA antibody**. ST: Seminiferous tubules. Proliferating cells with red nuclei (arrows) in basal layer of the germinal epithelium.

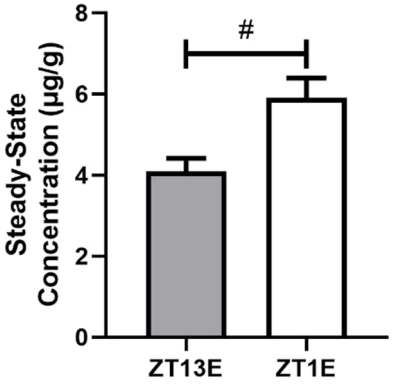

Fig. 4. Dosing-time dependent steady-state concentrations of everelimus in testis. Data are mean±SEM. ZT1E: Everolimus-treated mice at ZT1; ZT13E: Everolimus-treated mice at ZT13, $n = 7–8$ for each group. (ZT1E: 5.91±0.49, ZT13E: 4.09±0.66). Student-t-test ($^{\#}$ $p<0.05$).

Monitoring body weight in the course of the treatment provide us an index of the general health status of mice, which is important for the interpretation of reproductive effects. In general, body weight loss or reduction in weight gain may reflect various responses including treatment-induced anorexia, or systemic toxicity. Severe reductions in body weight may affect the male reproductive organs and reproductive function (Woldemeskel, 2017). Accordingly, in our study marked body weight loss in mice treated with everolimus at ZT1 was accompanied by the severe testicular damage.

Organ weight changes are very sensitive indicators of chemically induced toxicity in organs. In our study, liver, kidney and lung weights were significantly increased in everolimus treated mice at ZT1 as a sign of overall toxicity, while no apparent change was observed following treatment at ZT13. Testis weight can provide useful insight into the reproductive function of animals and may be helpful for reproductive risk assessment. A significant decrease or increase in testis weight measurements is indicative of a testicular toxicity and reproductive impairment (Michael et al., 2007; Woldemeskel, 2017). In our study, subacute everolimus treatment caused a decrease in the testis weights of mice at both ZT1 and ZT13. A diurnal variation in the susceptibility of testis to everolimus toxicity was demonstrated. Strikingly, reductions in the testis weights were significantly greater in mice treated with everolimus at ZT1 as compared to ZT13. Our first results give hints that the toxic effects of everolimus on the reproductive system are dosing time-dependent (circadian testicular toxicity). Germ cell depletion is the major cause of the decreased testis weight (Ilbey et al., 2009; Woldemeskel, 2017). Testicular weights reveal sensitivity to toxicity due to perturbations in rapidly dividing cells and physiology, and correlate well with histopathological changes (Michael et al., 2007). The reduction of 10% or higher in the organ weight measures is generally of toxic significance, in particular if accompanied by correlative macroscopic and microscopic findings (Woldemeskel, 2017).

It has been demonstrated that reproductive toxicity measurements including histopathology from the repeated dose toxicity studies are the most sensitive endpoints in predicting reproductive toxicity (Lanning et al., 2002). In our study, histopathological evaluation of testis tissues showed the prominent role of circadian timing in drug administration in male reproductive risk assessment, since we observed circadian time-dependent damage. Everolimus-induced histological changes on testes included vacuolization and atrophy of germinal epithelium, and loss of germinal cell attachment. There was a dramatic difference between ZT1 and ZT13-groups in the pathological morphology of testis, which was more evident when drug administered to mice at ZT1 than ZT13. It is known that impacts on germ cells disrupt the spermatogenesis. Spermatogenic cell population exhibited a drastic decline when everolimus administered at ZT1. The number of SPTs were notably decreased in ZT1 group. It has been stated that depletion of SPT in testes is responsible for low sperm count (Sinha et al., 2001). This data pointed out that the sperm reduction can be associated with decrease in the number of SPTs. Our findings regarding the low number of SPTs in ZT1E group have suggested that dosing time of everolimus (circadian timing) is significant for sperm production. Therefore, to decrease the testicular toxicity of everolimus and prevent the disruption of spermatogenesis, drug could be administered in the respective time of best tolerability to patients, providing a chronotherapy approach.

The molecular mechanisms by which mTOR inhibitors induce gonadal dysfunction and infertility still remain partly unknown. The stem cell factor (SCF)/c-kit tyrosine kinase system is one of the most important hormone-receptor signaling pathways essential for the proper development and maturation of functional germ cells and the maintenance of fertility. SCF/c-kit is involved in many functions including germ cell migration, cell adhesion, cellular proliferation and anti-apoptotic action in the testis (Framarino-Dei-Malatesta et al., 2013). c-kit-induced activation of PI3K is necessary for spermatogonial

proliferation and male fertility, and in testis mTOR inhibitor sirolimus plays a central inhibitory role in SCF/c-kit-dependent process in spermatogonia via PI3K/AKT/mTOR pathway (Feng et al., 2000). mTOR inhibitor everolimus thereby can abolish spermatogonial cell cycle progression and growth, leading to impairment in gonadal function.

The underlying mechanism of the circadian time-dependent testicular toxicity of everolimus appear to be complicated. However, a possible explanation for these circadian chronotolerance rhythms may arise from the circadian rhythmic pattern of the mTOR pathways. It has been shown that mTOR pathway is under the control of circadian clock in suprachiasmatic nucleus (SCN) in mice, and mTOR exhibit maximal activity during the subjective day (at ZT4), and minimal activity during the late subjective night (Cao et al., 2011). Since mTOR is a key regulator of spermatogonial proliferation, exposure time to mTOR inhibitor everolimus may raise the severity of male gonadal toxicity.

Spermatogenesis in mammals is a dynamic process. The first stage of spermatogenesis involves production of spermatocytes starting with the proliferation of spermatogonium situated in basal layer of the germinal epithelium found in serminiferous tubule wall. The second stage is to formation of haploid cells, the spermatids, via meiotic divisions of spermatocytes and the last stage is transformation of spermatid to sperm (Cole, 2016). Maintenance of adult spermatogenesis is related to resident A-type undifferentiated spermatogonia cell population that is able to both self-renewal and produce differentiating progeny (Mäkelä and Hobbs, 2019). Therefore, mitotic activity of spermatogonium is the major phenomenon for well-organized spermatogenesis. In our present study, proliferating cell population of basal cell layer of the germinal epithelium in mice treated with everolimus at ZT1 (ZT1E group) was markedly decreased when compared to control groups and ZT13 experimental group (ZT13E). The distribution of proliferative cells in the germinal epithelium did not evidently change in everolimus treated-group at ZT13 and in control groups. Circadian rhythmicity in cell division has been proved in the actively proliferating healthy tissues of rodents including gonads, gastrointestinal tract, bone marrow, and epidermis as well as in tumor cells. This circadian cell division accounts in part for the circadian varying sensitivity of healthy target tissues to anticancer agents (i.e. chronotoxicity/chronotolerance) (Sulli et al., 2019). Thus, chronotoxicological studies appear to be essential in determining the increased sensitivity to adverse effects and toxicities of drugs in the body in relation to administration time in a day, as shown in our current study. Our study revealed that toxicity to reproductive system induced by everolimus as shown by testicular damage was profoundly reduced when drug was administered at ZT13, i.e. early activity-span of mice. Our findings suggested that the drug administration time is important for proper spermatogenesis.

Circadian pharmacokinetics (or called chronopharmacokinetics) may be one of the main sources of dosing time-dependent drug effects and contribute to the difference in the apparent sensitivity to drug-induced toxicity in mammals (Ruben et al., 2019). To consider the pharmacokinetic mechanisms of this observed chronotoxicity, we examined everolimus levels in the testis tissues. Everolimus showed dosing time-dependent distribution profile in testis tissue. Testis concentrations of everolimus indicated a pronounced variation, which was greater in mice treated at ZT1 as compared to ZT13. Dosing-time dependent difference in everolimus testis concentrations and the apparent sensitivity to everolimus-induced testicular toxicity at ZT1 may be partly explained by circadian pharmacokinetics of everolimus. Biological defense factors drug metabolizing enzymes and drug efflux transporters show diurnal variation in their gene expression levels and activities (Ando et al., 2005; Lu et al., 2013; Okyar et al., 2019; Pala Kara et al., 2021; Zhang et al., 2009). These variations can induce the different sensitivity to many xenobiotics and drugs in a day. Thus, drug efficacy, tolerability to adverse effects and target organ toxicity may be modified depending on drug administration time (Dallmann et al., 2016; Levi et al., 2010; Ozturk et al., 2017). Everolimus is predominantly metabolized by the cytochrome P450 (CYP) enzymes CYP3A4 and CYP3A5 in the liver and intestinal wall (Booth, 2010; Kirchner et al., 2004). It is also a substrate of the efflux transporter P-glycoprotein (P-gp) (Chu et al., 2009; Crowe and Lemaire, 1998). P-gp genes (*Abcb1a* and *Abcb1b,* the rodent homologues of P-gp) were expressed in a circadian manner with a peak at ZT12–16 in the liver and intestine of C57BL/6 J mice (Ando et al., 2005). 2.9 fold fluctuation in P-gp expression was observed, with a maximal at ZT17 and trough at ZT1 in the liver of C57BL/6 J male mice (Zhang et al., 2009). Protein levels of P-gp in the intestine also exhibited a clear 24 h rhythm, with an increasing pattern towards the end of the light phase, a peak at the beginning of the dark phase, and a trough at the onset of the light phase (Ando et al., 2005; Okyar et al., 2019; Pala Kara et al., 2021). Likewise, CYP450 enzyme Cyp3a11 (homologue to human CYP3A4) showed the highest mRNA levels at ZT21 and the lowest at ZT1 in the liver of C57BL/6 J mice (Lu et al., 2013; Zhang et al., 2009). Therefore, we can suggest that the circadian rhythms of P-gp and CYP3A could modify the susceptibility of the organism to everolimus depending on the dosing-time, and thus may contribute to the chronotoxicity of this drug on the reproductive system observed as testicular atrophy in mice. In the current study the greater sensitivity of mice to everolimus at ZT1 may be translated into the poorest detoxification capability at this circadian time. Modulation of everolimus administration time according to the circadian rhythms in P-gp and CYP3A may be a useful strategy to improve the pharmacological and toxicological profile of this drug.

The blood-testis barrier (BTB), which is constituted by adjacent Sertoli cells is one of the tightest blood-tissue barriers in mammals including rodents and humans (Su et al., 2011). Efflux transporter P-gp (*Mdr1a*) is highly expressed in this tight junction of testis and serves as a gatekeeper to limit the entry of a wide variety of xenobitoics and drugs to germ cells by pumping back into the blood to protect them from harmful substances (Su et al., 2011). Immuno-histochemical studies have shown that P-gp is localized at the luminal (apical) side of the capillary endothelial cells as in the blood-brain barrier, as well as detected in Sertoli cells, Leyding cells, peritubular myoid cells, and late spermatids (Su et al., 2011). Experimental studies with P-gp knock-out mice (mdr1a$^{-/-}$/mdr1b$^{-/-}$ mice) confirm that P-gp maintain higher xenobiotic concentrations in the testes than wild-types (Balayssac et al., 2005). The circadian pattern of P-gp activity in different organs may affect the tissue distribution of drugs which are effluxed by this transporter (Ando et al., 2005; Pácha et al., 2021; Zhang et al., 2021). In a recent study, it has been shown that efflux of xenobiotics by the blood-brain barrier oscillates in mice, with highest levels during the active phase (darkness period, peak at ZT14) and lowest during the resting phase (light period, trough at ZT2) (Zhang et al., 2021). However, it is not known whether P-gp function in the testis is constant or it fluctuates during the day. There have been no studies to date investigating the circadian rhythmic pattern of P-gp or other drug transporters in the testes. Although the experimental evidence of circadian gene expression/activity of P-gp in testis tissue is lacking, we cannot exclude the possibility of the involvement of P-gp in the observed diurnal variability in the distribution of everolimus. The highest testis levels of everolimus at ZT1 may be corresponded to that of lowest efflux function in BTB.

Chronopharmacokinetics and chronotoxicity of many drugs, especially drugs used in cancer treatment, have been studied in both experimental animals and humans (Dallmann et al., 2016; Lévi et al., 2010; Ohdo et al., 2019; Ozturk et al., 2017). In a recent study, oxaliplatin-induced myelotoxicity has been found to be dosing-time dependent. It has been shown that circadian expression and function of efflux transporter MRP4 (Multi-drug resistance associated protein 4) in bone marrow cells of mice has caused administration time-dependent changes in drug disposition and target organ toxicity. Lower oxaliplatin accumulation in bone marrow cells and consistently lower myelotoxicity have been detected in mice after injection at the mid-dark phase, during which the expression levels of MRP4 increased (Kato et al., 2020). Significant dosing time-dependent toxicity was reported with fenvalerate

on reproductive function of male rats (Qin et al., 2012). Better tolerance by mice treated during the light-resting span was observed with lowest mean body weight loss, neutropenia and fastest hematology recovery (Filipski et al., 2004). Carboplatin treatment at 06.00 was associated with significantly greater thrombocytopenia than at 18.00 in patients with advanced ovarian carcinoma (Kerr et al., 1990). Thus, chrono-modulated approaches are of clinical interest since it appears to provide an opportunity to optimize drug therapy especially for anti-cancer medications by maximizing their efficay and minimizing severe side effects and toxicity.

It has been reported that tolerability of many anticancer drugs may be modified by circadian timing up to 10-fold in preclinical and clinical studies. Strikingly, optimal antitumor efficacy usually result from drug administration at the circadian time when the drug tolerability was best (Filipski et al., 2014; Lévi et al., 2010; Li et al., 2005). A study by Okazaki et al. (2014) has reported that the survival rate of tumor-bearing mice was higher when everolimus was administered at ZT12 (~ZT13) than ZT0 (~ZT1) in renal carcinoma model. In a word, there was a good accordance between our results and that of Okazaki et al. where they showed that everolimus dosing time at the beginning of the dark span seemed to be optimal, corresponded to the longest survival span. Since our results showed that everolimus tolerability in healthy mice was better at ZT13 as compared to ZT1, we can suggest that improved efficacy was observed in tumor-bearing mice when everolimus was given near its respective time of best tolerability (in terms of reproductive toxicity).

As a conclusion, we may suggest that the severity of everolimus-induced toxicity in testes varies significantly according to the administration time along the 24-h time scale. The findings are considerable in terms of revealing the dosing time-dependent testicular toxicity of everolimus in mice, which has been greater when everolimus administered at early rest-span (daytime-ZT1, i.e. the worst time) than early activity-span (nighttime-ZT13, i.e. the best time). Our findings support the concept of everolimus chronotherapy for minimizing drug-induced toxic effects on reproductive system and increasing the tolerability of everolimus, by optimizing the dosing schedule in male patients at reproductive age, under the risk of infertility on long-term use of everolimus. Yet, further studies are needed to understand the underlying mechanisms for this diurnal variation in the severity of everolimus-induced testicular toxicity, and clinical trials to address this issue should be urged.

Funding

The present work was supported by the Research Fund of Istanbul University (Project No. N-41109) and the Research Fund of Bezmialem Vakif University (Project No. 6.2015/25).

Author contributions

Narin Ozturk: Conceptualization, Investigation, Funding acquisition, Writing- Original draft preparation **Dilek Ozturk Civelek:** Investigation, Formal Analysis, Writing- Original draft preparation **Serap Sancar:** Investigation, Formal Analysis, Writing- Original draft preparation **Engin Kaptan:** Investigation, Formal Analysis, Writing- Original draft preparation **Zeliha Pala Kara:** Investigation, Writing- Original draft preparation **Alper Okyar:** Conceptualization, Funding acquisition, Writing- Reviewing and Editing.

Declaration of Competing Interest

The authors are not aware of any affiliations, memberships, funding, or financial holdings that might be perceived as affecting the objectivity of this study.

References

Ando, H., Yanagihara, H., Sugimoto, K.I., Hayashi, Y., Tsuruoka, S., Takamura, T., Kaneko, S., Fujimura, A., 2005. Daily rhythms of P-glycoprotein expression in mice. Chronobiol. Int. 22, 655–665. https://doi.org/10.1080/07420520500180231.

Balayssac, D., Authier, N., Cayre, A., Coudore, F., 2005. Does inhibition of P-glycoprotein lead to drug-drug interactions? Toxicol. Lett. 156, 319–329. https://doi.org/10.1016/j.toxlet.2004.12.008.

Bicker, J., Alves, G., Falcão, A., Fortuna, A., 2020. Timing in drug absorption and disposition: the past, present, and future of chronopharmacokinetics. Br. J. Pharmacol. 177, 2215–2239. https://doi.org/10.1111/bph.15017.

Binkhorst, L., Kloth, J.S.L., de Wit, A.S., de Bruijn, P., Lam, M.H., Chaves, I., Burger, H., van Alphen, R.J., Hamberg, P., van Schaik, R.H.N., Jager, A., Koch, B.C.P., Wiemer, E.A.C., van Gelder, T., van der Horst, G.T.J., Mathijssen, R.H.J., 2015. Circadian variation in tamoxifen pharmacokinetics in mice and breast cancer patients. Breast Cancer Res. Treat. 152, 119–128. https://doi.org/10.1007/s10549-015-3452-x.

Boobes, Y., Bernieh, B., Saadi, H., Hakim, M.R.Al, Abouchacra, S., 2010. Gonadal dysfunction and infertility in kidney transplant patients receiving sirolimus. Int. Urol. Nephrol. 42, 493–498. https://doi.org/10.1007/s11255-009-9644-8.

Booth, J., Robeva, A., Rosamilia, M., 2010. Novartis Afinitor®/Votubia® (RAD001) Investigator's Brochure, 10th edition. Novartis Pharmaceutical Corporation, Switzerland.

Cao, R., Anderson, F.E., Jung, Y.J., Dziema, H., Obrietan, K., 2011. Circadian regulation of mammalian target of rapamycin signaling in the mouse suprachiasmatic nucleus. Neuroscience 181, 79–88. https://doi.org/10.1016/j.neuroscience.2011.03.005.

Chen, Y., Zhang, Zhi, Lin, Y., Lin, H., Li, M., Nie, P., Chen, Lizhong, Qiu, J., Lu, Y., Chen, Linqiang, Xu, B., Lin, W., Zhang, J., Du, H., Liang, J., Zhang, Zhiwei, 2013. Long-term impact of immunosuppressants at therapeutic doses on male reproductive system in unilateral nephrectomized rats: a comparative study. Biomed Res. Int. 690382 https://doi.org/10.1155/2013/690382, 2013.

Chu, C., Abbara, C., Noël-Hudson, M.S., Thomas-Bourgneuf, L., Gonin, P., Farinotti, R., Bonhomme-Faivre, L., 2009. Disposition of everolimus in mdr1a-/1b- mice and after a pre-treatment of lapatinib in Swiss mice. Biochem. Pharmacol. 77, 1629–1634. https://doi.org/10.1016/j.bcp.2009.02.013.

Cole, L.A., 2016. Biology of life: biochemistry, Physiology and Philosophy, 1st Ed. Academic Press, London, United Kingdom.

Crowe, A., Lemaire, M., 1998. In vitro and in situ absorption of SDZ-RAD using a human intestinal cell line (Caco-2) and a single pass perfusion model in rats: comparison with rapamycin. Pharm. Res. 15, 1666–1672. https://doi.org/10.1023/A:1011940108365.

Dallmann, R., Okyar, A., Lévi, F., 2016. Dosing-time makes the poison: circadian regulation and pharmacotherapy. Trends Mol. Med. 22, 430–445. https://doi.org/10.1016/j.molmed.2016.03.004.

Deutsch, M.A., Kaczmarek, I., Huber, S., Schmauss, D., Beiras-Fernandez, A., Schmoeckel, M., Ochsenkuehn, R., Meiser, B., Mueller-Hoecker, J., Bruno Reichart, B., 2007. Sirolimus-associated infertility: case report and literature review of possible mechanisms. Am. J. Transplant. 7, 2414–2421. https://doi.org/10.1111/j.1600-6143.2007.01929.x.

Fasolo, A., Sessa, C., 2008. mTOR inhibitors in the treatment of cancer. Expert Opin. Investig. Drugs. 17, 1717–1734. https://doi.org/10.1517/13543784.17.11.1717.

Feng, L.X., Ravindranath, N., Dym, M., 2000. Stem cell factor/c-kit up-regulates cyclin D3 and promotes cell cycle progression via the phosphoinositide 3-kinase/p70 S6 kinase pathway in spermatogonia. J. Biol. Chem. 275, 25572–25576. https://doi.org/10.1074/jbc.M002218200.

Filipski, E., Berland, E., Ozturk, N., Guettier, C., van der Horst, G.T.J., Lévi, F., Okyar, A., 2014. Optimization of irinotecan chronotherapy with P-glycoprotein inhibition. Toxicol. Appl. Pharmacol. 274, 471–479. https://doi.org/10.1016/j.taap.2013.12.018.

Filipski, E., Lemaigre, G., Liu, X.H., Méry-Mignard, D., Mahjoubi, M., Lévi, F., 2004. Circadian rhythm of irinotecan tolerability in mice. Chronobiol. Int. 21, 613–630. https://doi.org/10.1081/CBI-120040183.

Framarino-Dei-Malatesta, M., Derme, M., Manzia, T.M., Iaria, G., De Luca, L., Fazzolari, L., Napoli, A., Berloco, P., Patel, T., Orlando, G., Tisone, G., 2013. Impact of mtor-i on fertility and pregnancy: state of the art and review of the literature. Expert Rev. Clin. Immunol. 9, 781–789. https://doi.org/10.1586/1744666X.2013.824243.

Huyghe, E., Zairi, A., Nohra, J., Kamar, N., Plante, P., Rostaing, L., 2007. Gonadal impact of target of rapamycin inhibitors (sirolimus and everolimus) in male patients: an overview. Transpl. Int. 20, 305–311. https://doi.org/10.1111/j.1432-2277.2006.00423.x.

Huynh, H., Pierce Chow, K.H., Soo, K.C., Toh, H.C., Choo, S.P., Foo, K.F., Poon, D., Ngo, V.C., Tran, E., 2009. RAD001 (everolimus) inhibits tumour growth in xenograft models of human hepatocellular carcinoma. J. Cell. Mol. Med. 13, 1371–1380. https://doi.org/10.1111/j.1582-4934.2008.00364.x.

Ilbey, Y.O., Ozbek, E., Simsek, A., Otunctemur, A., Cekmen, M., Somay, A., 2009. Potential chemoprotective effect of melatonin in cyclophosphamide- and cisplatin-induced testicular damage in rats. Fertil. Steril. 92, 1124–1132. https://doi.org/10.1016/j.fertnstert.2008.07.1758.

Innominato, P.F., Ballesta, A., Huang, Q., Focan, C., Chollet, P., Karaboué, A., Giacchetti, S., Bouchahda, M., Adam, R., Garufi, C., Lévi, F.A., 2020. Sex-dependent least toxic timing of irinotecan combined with chronomodulated chemotherapy for metastatic colorectal cancer: randomized multicenter EORTC 05011 trial. Cancer Med 9 (12), 4148–4159. https://doi.org/10.1002/cam4.3056.

Iwata, K., Aizawa, K., Sakai, S., Jingami, S., Fukunaga, E., Yoshida, M., Hamada, A., Saito, H., 2011. The relationship between treatment time of gemcitabine and

development of hematologic toxicity in cancer patients. Biol. Pharm. Bull. 34, 1765–1768. https://doi.org/10.1248/bpb.34.1765.
Kato, M., Tsurudome, Y., Kanemitsu, T., Yasukochi, S., Kanado, Y., Ogino, T., Matsunaga, N., Koyanagi, S., Ohdo, S., 2020. Diurnal expression of MRP4 in bone marrow cells underlies the dosing-time dependent changes in the oxaliplatin-induced myelotoxicity. Sci. Rep. 10, 13484. https://doi.org/10.1038/s41598-020-70321-6.
Kerr, D.J., Lewis, C., O'Neil, B., Lawson, N., Blackie, R.G., Newell, D.R., Boxall, F., Cox, J., Rankin, E.M., Kaye, S.B., 1990. The myelotoxicity of carboplatin is influenced by the time of its administration. Hematol. Oncol. 8, 59–63. https://doi.org/10.1002/hon.2900080108.
Kirchner, G.I., Meier-Wiedenbach, I., Manns, M.P., 2004. Clinical Pharmacokinetics of Everolimus. Clin. Pharmacokinet. 43, 83–95. https://doi.org/10.2165/00003088-200443020-00002.
Klawitter, J., Nashan, B., Christians, U., 2015. Everolimus and sirolimus in transplantation-related but different. Expert Opin. Drug Saf. 14, 1055–1070. https://doi.org/10.1517/14740338.2015.1040388.
Lanning, L.L., Creasy, D.M., Chapin, R.E., Mann, P.C., Barlow, N.J., Regan, K.S., Goodman, D.G., 2002. Recommended approaches for the evaluation of testicular and epididymal toxicity. Toxicol. Pathol. 30, 507–520. https://doi.org/10.1080/01926230290105695.
Lebwohl, D., Anak, Ö., Sahmoud, T., Klimovsky, J., Elmroth, I., Haas, T., Posluszny, J., Saletan, S., Berg, W., 2013. Development of everolimus, a novel oral mTOR inhibitor, across a spectrum of diseases. Ann. N. Y. Acad. Sci. 1291, 14–32. https://doi.org/10.1111/nyas.12122.
Leighton, J.K., Saber, H., Lee, H., 2009. Memorandum Afinitor (everolimus). Pharmacology/Toxicology Review and Evaluation. Center for Drug Evaluation and Research, Food and Drug Administration. NDA. No: 22-334. https://www.accessdata.fda.gov/drugsatfda_docs/nda/2009/022334s000_PharmR. pdf.
Lévi, F., Okyar, A., Dulong, S., Innominato, P.F., Clairambault, J., 2010. Circadian timing in Cancer treatments. Annu. Rev. Pharmacol. Toxicol. 50, 377–421. https://doi.org/10.1146/annurev.pharmtox.48.113006.094626.
Li, X.M., Tanaka, K., Sun, J., Filipski, E., Kayitalire, L., Focan, C., Levi, F., 2005. Preclinical relevance of dosing time for the therapeutic index of gemcitabine-cisplatin. Br. J. Cancer 92, 1684–1689. https://doi.org/10.1038/sj.bjc.6602564.
Lu, Y.F., Jin, T., Xu, Y., Zhang, D., Wu, Q., Zhang, Y.K.J., Liu, J., 2013. Sex differences in the circadian variation of cytochrome p450 genes and corresponding nuclear receptors in mouse liver. Chronobiol. Int. 30, 1135–1143. https://doi.org/10.3109/07420528.2013.805762.
Mäkelä, J.A., Hobbs, R.M., 2019. Molecular regulation of spermatogonial stem cell renewal and differentiation. Reproduction 185, 169–187. https://doi.org/10.1530/REP-18-0476.
Manito, N., Delgado, J.F., Crespo-Leiro, M.G., González-Vílchez, F., Almenar, L., Arizón, J.M., Díaz, B., Fernández-Yáñez, J., Mirabet, S., Palomo, J., Rodríguez Lambert, J.L., Roig, E., Segovia, J., 2010. Clinical recommendations for the use of everolimus in heart transplantation. Transplant. Rev. 24, 129–142. https://doi.org/10.1016/j.trre.2010.01.005.
Meistrich, M., Hess, R.A., 2013. Assessment of spermatogenesis through staging of seminiferous tubules. Methods Mol Biol 927, 299–307. https://doi.org/10.1007/978-1-62703-038-0_27.
Michael, B., Yano, B., Sellers, R.S., Perry, R., Morton, D., Roome, N., Johnson, J.K., Schafer, K., Pitsch, S., 2007. Evaluation of organ weights for rodent and non-rodent toxicity studies: a review of regulatory guidelines and a survey of current practices. Toxicol. Pathol. 35, 742–750. https://doi.org/10.1080/01926230701595292.
Mohawk, J.A., Green, C.B., Takahashi, J.S., 2012. Central and peripheral circadian clocks in mammals. Annu. Rev. Neurosci. 35, 445–462. https://doi.org/10.1146/annurev-neuro-060909-153128.
Ohdo, S., Koyanagi, S., Matsunaga, N., 2019. Chronopharmacological strategies focused on chrono-drug discovery. Pharmacol. Ther. 202, 72–90. https://doi.org/10.1016/j.pharmthera.2019.05.018.
Okazaki, H., Matsunaga, N., Fujioka, T., Okazaki, F., Akagawa, Y., Tsurudome, Y., Ono, M., Kuwano, M., Koyanagi, S., Ohdo, S., 2014. Circadian regulation of mTOR by the ubiquitin pathway in renal cell carcinoma. Cancer Res 74 (2), 543–551. https://doi.org/10.1158/0008-5472.CAN-12-3241.
Okyar, A., Piccolo, E., Ahowesso, C., Filipski, E., Hossard, V., Guettier, C., La Sorda, R., Tinari, N., Iacobelli, S., Lévi, F., 2011. Strain- and sex-dependent circadian changes in abcc2 transporter expression: implications for irinotecan chronotolerance in mouse ileum. PLoS One 6 (6), e20393. https://doi.org/10.1371/journal.pone.0020393.
Okyar, A., Kumar, S.A., Filipski, E., Piccolo, E., Ozturk, N., Xandri-Monje, H., Pala, Z., Abraham, K., Gomes, A.R.G., de, J., Orman, M.N., Li, X.-.M., Dallmann, R., Lévi, F., Ballesta, A., 2019. Sex-, feeding-, and circadian time-dependency of P-glycoprotein expression and activity - implications for mechanistic pharmacokinetics modeling. Sci. Rep. 9, 10505. https://doi.org/10.1038/s41598-019-46977-0.
Ozturk, N., Okyar, A., Li, X.M., Lévi, F., 2014. The circadian timing system as a toxicity target of anticancer mTOR inhibitor everolimus in mice. Basic Clin Pharmacol Toxicol 115, 318.
Ozturk, N., Ozturk, D., Kavakli, I.H., Okyar, A., 2017. Molecular aspects of circadian pharmacology and relevance for cancer chronotherapy. Int. J. Mol. Sci. 18, 2168. https://doi.org/10.3390/ijms18102168.
Ozturk, N., Ozturk, D., Pala-Kara, Z., Kaptan, E., Sancar-Bas, S., Ozsoy, N., Cinar, S., Deniz, G., Li, X.-.M., Giacchetti, S., Lévi, F., Okyar, A., 2018. The immune system as a chronotoxicity target of the anticancer mTOR inhibitor everolimus. Chronobiol. Int. 35, 705–718. https://doi.org/10.1080/07420528.2018.1432632.
Pácha, J., Balounová, K., Soták, M., 2021. Circadian regulation of transporter expression and implications for drug disposition. Expert Opin. Drug Metab. Toxicol. 1–15. https://doi.org/10.1080/17425255.2021.1868438.
Pala Kara, Z., Ozturk Civelek, D., Ozturk, N., Okyar, A., 2021. The effects of P-glycoprotein inhibitor zosuquidar on the sex and time-dependent pharmacokinetics of parenterally administered talinolol in mice. Eur. J. Pharm. Sci. 156, 105589 https://doi.org/10.1016/j.ejps.2020.105589.
Qin, F., Yuan, H., Chen, L., Jiang, B., Tong, J., Zhang, J., 2012. Chronotoxicology of fenvalerate on the male rats reproductive system. Journal of hygiene research, 41 (6), 905–910. PMID: 23424865.
Rovira, J., Diekmann, F., Ramírez-Bajo, M.J., Bañón-Maneus, E., Moya-Rull, D., Campistol, J.M., 2012. Sirolimus-associated testicular toxicity: detrimental but reversible. Transplantation 93, 874–879. https://doi.org/10.1097/TP.0b013e31824bf1f0.
Ruben, M.D., Smith, D.F., FitzGerald, G.A., Hogenesch, J.B., 2019. Dosing time matters. Science 365, 547–549. https://doi.org/10.1126/science.aax7621.
Sancar, A., Van Gelder, R.N., 2021. Clocks, cancer, and chronochemotherapy. Science 371, 6524. https://doi.org/10.1126/science.abb0738.
Sinha, N., Adhikari, N., Saxena, D.K., 2001. Effect of endosulfan during fetal gonadal differentiation on spermatogenesis in rats. Environ Toxicol Pharmacol 10, 29–32. https://doi.org/10.1016/s1382-6689(01)00066-7.
Su, L., Mruk, D.D., Cheng, C.Y., 2011. Drug transporters, the blood-testis barrier, and spermatogenesis. J. Endocrinol. 208, 207–223. https://doi.org/10.1677/JOE-10-0363.
Sulli, G., Lam, M.T.Y., Panda, S., 2019. Interplay between Circadian Clock and Cancer: new Frontiers for Cancer Treatment. Trends in Cancer 5, 475–494. https://doi.org/10.1016/j.trecan.2019.07.002.
Woldemeskel, M., 2017. Toxicologic pathology of the reproductive system. Reproductive and Developmental Toxicology. Academic Press, pp. 1209–1241. https://doi.org/10.1016/B978-0-12-804239-7.00064-0.
Zhang, S.L., Lahens, N.F., Yue, Z., Arnold, D.M., Pakstis, P.P., Schwarz, J.E., Sehgal, A., 2021. A circadian clock regulates efflux by the blood-brain barrier in mice and human cells. Nat. Commun. 12, 617. https://doi.org/10.1038/s41467-020-20795-9.
Zhang, Y.K.J., Yeager, R.L., Klaassen, C.D., 2009. Circadian expression profiles of drug-processing genes and transcription factors in mouse liver. Drug Metab. Dispos. 37, 106–115. https://doi.org/10.1124/dmd.108.024174.